Chemokines IL-8, GROα, MCP-1, IP-10, and Mig Are Sequentially and Differentially Expressed During Phase-Specific Infiltration of Leukocyte Subsets in Human Wound Healing

Eva Engelhardt,* Atiye Toksoy,*
Matthias Goebeler,* Sebastian Debus,†
Eva-Bettina Bröcker,* and Reinhard Gillitzer*

From the Departments of Dermatology* and Surgery,† University of Würzburg Medical School, Würzburg, Germany

Healing of cutaneous wounds requires a complex integrated network of repair mechanisms, including the action of newly recruited leukocytes. Using a skin repair model in adult humans, we investigated the role chemokines play in sequential infiltration of leukocyte subsets during wound healing. At day 1 after injury, the C-X-C chemokines IL-8 and growth-related oncogene α are maximally expressed in the superficial wound bed and are spatially and temporally associated with neutrophil infiltration. IL-8 and growth-related oncogene α profiles also correlate with keratinocyte migration and subsequently subside after wound closure at day 4. Macrophage infiltration reaches the highest levels at day 2 and is paralleled by monocyte chemoattractant protein-1 mRNA expression in both the basal layer of the proliferative epidermis at the wound margins and mononuclear cells in the wound area. Other monocyte-attracting chemokines such as monocyte chemoattractant protein-3, macrophage inflammatory protein-1α and -1β, RANTES, and I309 are undetectable. At day 4, perivascular focal lymphocyte accumulation correlates with strong focal expression of the C-X-C chemokines Mig and IP-10. Our results suggest that a dynamic set of chemokines contributes to the spatially and temporally different infiltration of leukocyte subsets and thus integrates the inflammatory and reparative processes during wound repair. *(Am J Pathol 1998, 153:1849–1860)*

Undisturbed wound healing follows a course that typically starts with blood clotting, activation of thrombocytes, and, later, immigration of inflammatory cells into the provisional matrix of the wounded region.[1,2] There is increasing evidence that different subpopulations of inflammatory cells are important during the catabolic phase of healing as well as anabolic phase.[3] Initially, neutrophils accumulate in the damaged tissue, where they form a first line of defense against local infections and aid initial debridement by synthesizing and secreting hydrolases and reactive oxygen intermediates.[2] Afterwards, accumulating macrophages enhance the debridement[4] and present antigens to initiate specific immune responses. In addition, macrophages are important producers for a battery of growth factors such as platelet-derived growth factor (PDGF), transforming growth factor β (TGF-β), and basic fibroblast growth factor (bFGF).[3,5] These factors stimulate the synthesis of extracellular matrix components produced by fibroblasts and the ingrowth of blood vessels from the surrounding tissue. More recently, it has become evident that lymphocytes, besides acting as immunological effector cells, are also capable of producing particular growth factors such as bFGF and leukocyte-derived growth factor.[6,7] Their later appearance in the wound area may further tissue formation and remodeling of the tissue components.

Consequently, analyzing the mechanisms responsible for the phase-specific and spatially differential recruitment of leukocyte subsets is a prerequisite for understanding both normal and pathological (ie, delayed or hypertrophic) wound repair. Besides adhesion molecules,[8,9] the targeting processes of extravasation and tissue homing depend on chemoattractants such as chemokines.[10] By virtue of their target-cell specificity, chemokines selectively mediate the regionally specific recruitment of neutrophils, macrophages, and lymphocytes. C-X-C chemokines such as IL-8,[11–13] growth-related oncogene α (GROα),[14,15] and epithelial derived neutrophil attractant-78 amino acids (ENA-78)[16] containing the glutamin acid-leucine-arginine motif[17] preferentially attract neutrophils and possibly lymphocytes.[18,19] The C-X-C chemokines, such as monokine induced by interferon-γ (Mig)[20–22] and interferon-γ-inducible protein-10 (IP-10),[23] which lack the glutamin acid-leucine-arginine motif, selectively attract lymphocytes.[24–26] The

C-C chemokines are the second subfamily of chemokines which include monocyte chemoattractant protein-1 (MCP-1),[27,28] macrophage inflammatory protein-1α and β (MIP-1α and β),[29,30] I309[31] and the "regulated on activation normal T cells expressed and secreted" (RANTES).[32] Chemokines from this family show a partly overlapping specificity for macrophages, lymphocytes,[33,34] and non-neutrophil granulocytes.[35]

So far, the role of individual chemokines during wound healing has been studied mainly in rodent models.[36–38] DiPietro and colleagues found maximum levels of JE mRNA, the murine homologue of MCP-1, at 12–24 hours after wounding, followed by a peak of macrophage infiltration 1–2 days later.[38] More recently, DiPietro also detected MIP-1α as a critical mediator of monocyte recruitment in murine wound repair.[36] However, it is not clear whether human and murine chemokine homologues exhibit similar functions *in vivo*, leaving open the question whether their physiological roles during inflammatory reactions are comparable. In view of these discrepancies and due to the lack of available chemokine reagents for animal models with a comparable morphology to human skin (eg, pigs, rabbits, or guinea pigs), we decided to focus on the role chemokines play in wound healing of adult human skin. Recently, expression of GROα and its receptor were studied in human wounds at days 2–12 after accidental burn injuries.[39] The authors observed immunoreactivity to GROα in exudates and granulation tissue, which was associated with inflammatory infiltrates from days 3–12 after injury. Moreover, expression of the CXC-receptor 2 (CXCR2), previously designated as the IL-8 receptor B, was detected early after wounding in undifferentiated keratinocytes.[39] However, with the exception of GRO and CXCR2 immunoreactivity in burn wounds, little is known about the temporal and spatial appearance of chemokines and their influences on re-epithelialization and angiogenesis during normal human wound healing. In this study, we investigated the role of neutrophil-, macrophage- and lymphocyte-specific chemokines during human wound healing in a standardized manner, using incisional skin wounds of constant size, constant localization, and defined time intervals in adult volunteers.

As several studies have demonstrated, *in vivo* data on chemokine mRNA expression are highly representative of the presence of their respective target cells.[38,40–44] In contrast, chemokine labeling by immunohistochemical measures is less reliable, because the attachment of immunoreactive epitopes to the extracellular matrix leads to a high background signal. This problem is of particular relevance in early wound healing lesions with the strong deposition of fibrin and fibrinogen. For this reason we used *in situ* hybridization to identify and localize chemokine mRNA expression and immunohistochemistry to detect the distribution of leukocyte subsets.

We demonstrate in this study that during normal healing of adult skin wounds, distinct repertoires of chemokines are expressed. These repertoires correlate spatially and temporally with the phase-specific recruitment and trafficking of neutrophils, macrophages, and lymphocytes.

Materials and Methods

Provocation of Incisional Wounds

After obtaining informed consent from each of 14 healthy adult volunteers of Caucasian origin, incisions ($n = 4$–7) 5 mm deep and 5 mm long were made on the ulnar forearm. The volunteers were 8 women and 6 men ranging in age from 25–58 years (mean, 39.9 years). Pending collection of biopsy specimens after various time periods, wounds were covered with sterile dressing. The study was approved by the Ethics Commission at the University of Würzburg and performed according to the Declarations of Helsinki and Tokyo.

Biopsy Specimens

At defined time intervals after wounding (1, 2, 4, 7, 10, 14, and 21 days), 5-mm punch biopsies were obtained under local anesthesia. Biopsy specimens from healthy volunteers ($n = 6$) of nonwounded skin were used as controls. The tissue samples were placed in optimal cutting temperature compound (Tissue-Tek, Miles Scientific, Naperville, IL) immediately after excision, frozen, and stored at $-80°C$. Cryostat sections measuring 5 μm were prepared on gelatine-coated slides (Merck, Darmstadt, Germany) for immunohistology and on polyL-lysin-coated slides (Sigma, Deisenhofen, Germany) for *in situ* hybridization, respectively. After air-drying, sections were fixed in acetone (10 minutes at 4°C) for immunohistochemistry or in 4% paraformaldehyde/phosphate-buffered saline (PBS) for 20 minutes at room temperature (RT) for *in situ* hybridization.

Antibodies and Antisera

For immunohistological staining the following mouse mAbs were used at the indicated dilutions: anti-CD3 (1:100; Becton Dickinson, Sunnyvale, CA), reacting with the T cell receptor-associated CD3 antigen; anti-CD68 (1:1000; Dako, Hamburg, Germany), reacting with monocytes and macrophages; anti-neutrophil elastase (1:200; Dako), specific for neutrophils; MiB-1 (1:200; Dianova, Hamburg, Germany), detecting the Ki-67 proliferation antigen, EN4 (1:500; Sera Lab, Crawley Down, UK) specific for endothelial cells, anti-GROα (1:50; R+D Systems, Minneapolis, MN), anti-MCP-1 (1:50; R+D Systems), anti-MIP-1α (1:20; Promega, Madison, WI), and anti-RANTES (1:50; R+D Systems).

The following antisera were used: anti-Mig (rabbit antiserum, 1:200), raised against denatured human Mig (kindly provided by J. M. Farber, Laboratory for Clinical Investigation, National Institutes of Health, Bethesda, MD), and anti-IP-10 (goat antiserum, 1:500), raised against denatured human IP-10 (R+D Systems).

Biotin-conjugated sheep anti-mouse immunoglobulin (1:200; Amersham, Braunschweig, Germany), sheep anti-rabbit immunoglobulin (1:200; Jackson Immuno-Research, West Grove, PA) and sheep anti-goat immu-

noglobulin (1:200; Jackson ImmunoResearch) were used as the secondary antibody.

Immunohistology

For immunohistochemical staining a three-step streptavidin-biotin-peroxidase procedure was used.[40] First, slides were washed in 0.1% Tween 20 (Merck)/PBS (Sigma) and the nonspecific binding sites were blocked with 20% sheep serum (Dianova)/0.1% BSA (Merck)/PBS for 20 minutes at RT. Sections were then incubated with the primary antibody in 0.1% BSA/PBS at 4°C overnight. After intense washing in 0.1% Tween 20, the slides were incubated with the biotinylated sheep anti-mouse immunoglobulin as the secondary antibody for 1 hour at RT and, after further washing, were treated with streptABC-peroxidase (Dako) for 1 hour at RT. Labeling was visualized with 0.2 mg/ml 0.5% 3-amino-9-ethyl-carbazole (AEC) (Sigma) in *N,N*-dimethylformamide (Merck) and 0.005% H_2O_2 in acetate buffer (50 mmol/L, pH 5.0) at RT. Slides were finally counterstained with Papanicolaou's solution 1b (Merck). For control purposes, the first mAb was omitted and replaced by an isotype-matched antibody to control for nonspecificity.

In Situ *Hybridization*

Preparation of ^{35}S-labeled RNA Probes

The cDNA probes used for *in situ* hybridization were kindly provided by T. Yoshimura (National Cancer Institute, Frederick, MD; MCP-1), C. Müller (University of Bern, Bern, Switzerland; MCP-3 and ENA-78), Genetics Institute (Cambridge, MA; MIP-1α), T. Schall (DNAX, Palo Alto, CA; RANTES, MIP-1β), A. Anisowicz (Dana Farber Cancer Institute, Boston, MA; GROα), C. Weissmann (University of Zürich, Zürich, Switzerland; IL-8), R. Kulke (University of Kiel, Kiel, Germany; IP-10), J. Farber (National Cancer Institute, Bethesda, MD; Mig), and M. Krangel (Duke University Medical Center, Durham, NC; I309). Subcloning of specific DNA fragments was performed in vectors containing SP6/T7 (pGem 02, Promega, Madison, WI) or T3/T7 promoters (Bluescript, Stratagene, La Jolla, CA) according to standard protocols.[45] *In vitro* transcription of sense and antisense probes was performed as previously described.[40] Briefly, plasmid DNA was linearized with appropriate restriction enzymes. Then ^{35}S-labeled sense and antisense probes were obtained by *in vitro* transcription using SP6, T3, or T7 polymerases (Boehringer Mannheim, Mannheim, Germany) together with ATP, GTP, CTP (Boehringer) and [^{35}S]uridine triphosphate (Amersham) as substrates. Original linearized template cDNA was eliminated with deoxyribonuclease (Pharmacia, Uppsala, Sweden) and protein was removed by sequential phenol extraction steps. Then, alkaline hydrolysis of the ^{35}S-labeled RNA probes was performed for 30–50 minutes at 60°C in a carbonate buffer (pH 10.2) according to the formula: time (minutes) = $(L_0 - L_f)/0.11 \times L_0 \times L_f$ (L_0 = initial length in kb pairs, L_f = final length in kb pairs).[46] After several ethanol

precipitation steps, the radioactive riboprobe was adjusted to the specific activity of 1×10^6 cpm/μl in 0.01 mol/L Tris-HCl (pH 7.5), supplemented with 1 mmol/L EDTA.

Hybridization Procedure

In situ hybridization was done as previously described.[40] Paraformaldehyde-fixed cryostat sections were treated with proteinase K (Boehringer,) (1 μg/ml) for 30 minutes at 37°C, refixed in 4% paraformaldehyde in PBS (30 minutes, RT), acetylated with acetic anhydride in 0.1 mol/l triethanolamine (pH 8.0, 10 minutes), dehydrated in graded concentrations of alcohol, and air-dried. Afterwards, sections were overlaid with 20 μl of hybridization solution containing 50% formamide, 300 mmol/L NaCl, 20 mmol/L Tris-HCl (pH 8.0), 5 mmol/L EDTA, 1 $\times$ Denhardt's solution, 10% dextran sulfate, 100 mmol/L DTT, and 2×10^5 cpm heat-denatured radioactive sense or antisense probes per μl. The slides were mounted with coverslips, sealed, and hybridized at 46°C for 12–16 hours. Antisense and sense (negative control) probes were hybridized with at least two sections of the same biopsy. After hybridization, nonhybridized probes were removed by several high-stringency washing procedures with 50% formamide solution containing 2 $\times$ SSC buffer (Sigma) and 5 mmol/L EDTA at 54–57°C. To minimize the background signal, noncomplementary unhybridized single-stranded probe RNA was digested with RNase A (20 μg/ml) and RNase T1 (1 U/μl, Boehringer) for 30 minutes at 37°C. For autoradiography, slides were dipped in NTB-2 Kodak solution (1:2 in 800 mmol/L ammonium acetate), air-dried, and exposed for 1–5 weeks at 4°C. Slides were then counterstained with Papanicolaou's solution 1b.

As control tissues for chemokine expression, we used lesions of psoriasis (GROα, IL-8, IP-10, Mig, and MCP-1), leishmaniasis, leprosy (MIP-1α and MIP-1β), and lichen planus (RANTES).

Quantitation of Leukocyte Subsets, mRNA-Expressing Cells, and Vessel Growth

A Zeiss Axiophot microscope equipped with dark-field illumination (Carl Zeiss, Oberkochen, Germany) was used for evaluation and documentation. Positive cells were counted with an ocular square grid (Carl Zeiss) in one half of the symmetrical wound bed (magnifications, $\times$250 and $\times$400) and related to the total number of cells in the area. We examined 3 to 14 individual wounds for each time point. The average percentage of mRNA-expressing or -stained cells was determined and expressed as mean $\pm$ SEM. For evaluation of microvascular endothelium development, we counted the number of vessels in 2–3 random counting fields (magnification, $\times$200) within the wound bed and calculated the average number of vessels per counting field.
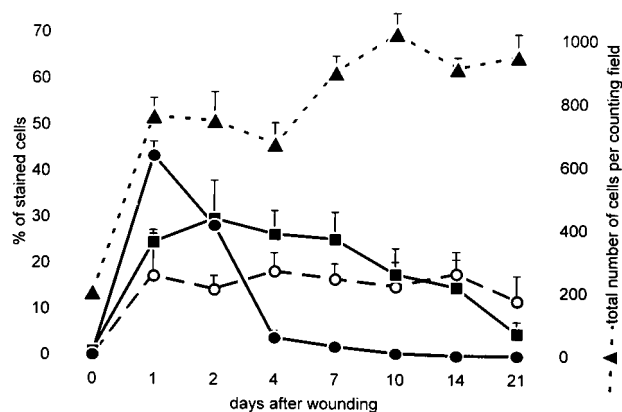
Figure 1. Time course of neutrophil, macrophage, and lymphocyte infiltration during human skin wound healing. Infiltrating leukocyte subsets were identified by immunostaining with mAbs anti-CD3 (○), anti-CD68 (●), and anti-neutrophil elastase (NE) (■), using a 3-step streptavidin-peroxidase method and 3-amino-9-ethyl-carbazole as substrate. The results are expressed as the mean percentage of stained cells per counting field (± SEM) of 3–10 lesion sections for each time point until day 21 after wounding. In addition, the total number of cells per counting field (± SEM) between day 0 and day 21 is shown (▲).

Results

Normal Healing of Adult Skin Wounds Is Accompanied by Spatially and Temporally Changing Patterns of Inflammatory Cells

In the first series of experiments, biopsies from incisional adult skin wounds 5 mm long and 5 mm deep taken at day 0, 1, 2, 4, 7, 10, 14, and 21 were evaluated for their histological features and time of wound closure, as determined by complete re-epithelialization of the wound gap with keratinocytes. In five of eleven individuals, wound closure was already completed after 48 hours (day 2), and in six patients closure took place between days 2 and 4. No obvious differences in wound healing between adult volunteers aged 20–30 ($n = 5$) and those aged 40–60 ($n = 4$) were seen. After day 4, a hypertrophic neo-epidermis developed over the previously denuded wound surface. Immunostaining with anti-leukocyte mAb for CD45$^+$ cells showed maximum leukocyte accumulation within the first 24 hours and a constant level until day 4. Afterwards, the number of CD45$^+$ cells slowly and constantly decline in the next 3 weeks (data not shown). However, the total number of cells after a dramatic increase between day 0 and day 1 remained rather constant (Figure 1), indicating that the slow decline of inflammatory cells after day 4 (wound closure in all lesions) is accompanied by the proliferation of resident cells as fibroblasts and endothelial cells. Immunohistological labeling with leukocyte subtype-specific mAbs revealed a strong dominance of NE$^+$ neutrophils during the first days, reaching a maximum level at day 1 (44 ± 3% of total cells; mean ± SEM) (Figure 1). The neutrophils concentrated in a rim of densely packed cells contained within the superficial part of the wound defect (Figure 2E), but their relative percentage decreased rapidly on wound closure (after days 2–4). In contrast to

neutrophils, CD68$^+$ macrophages reached their maximum level at day 2 (30 ± 8%) (Figure 1). The macrophages were distributed within and near the wounded area with preferential accumulation around dermal vessels. After day 2, the number of macrophages slowly declined. Lymphocytes were present at relatively constant levels (12–18%) (Figure 1) and, like macrophages, accumulated preferentially around superficial dermal vessels. The local appearance of lymphocytes was slightly delayed compared to neutrophils and macrophages. After day 14, however, lymphocytes constituted the major leukocyte subpopulation in the wound (Figure 1).

Re-epithelialization of Skin Wounds Is Associated with Keratinocyte Proliferation at the Epidermal Wound Edge and Neoangiogenesis

Staining with mAb MiB-1 showed that proliferation of keratinocytes was restricted to the epidermal compartment of the wound edge, whereas keratinocytes migrating from the margin into the wound bed were nonproliferating (data not shown). Only at later time points (days 7 and 10) was the proliferation of basal keratinocytes in the newly constituted acanthotic epidermis observed. This demonstrates that the mechanism of re-epithelialization is due to migration of keratinocytes that originate from undamaged epidermis surrounding the wound border. Staining of vessels by endothelial cell-specific mAb EN4 revealed an initial increase in density of vessels in the wound area. One day after wounding, an average number of 13.5 ± 2.3 (mean ± SEM) vessels per field was observed; this number nearly doubled by day 4 (21 ± 5). After reaching maximum vessel density at day 4, the number of vessels remained quite constant (19.5 ± 2.8 at day 7 and 19.1 ± 4.8 at day 10).

Expression of IL-8 and GROα mRNA during Healing of Deliberate Skin Wounds Is Temporally and Spatially Correlated with the Pattern of Neutrophil Infiltration

To better understand mechanisms of rapid neutrophil recruitment in cutaneous wounds, we analyzed the expression and microanatomical location of the neutrophil-attracting chemokines IL-8, GROα and ENA-78. Use of the radioactive IL-8 antisense (but not sense) probes demonstrates massive cell-associated hybridization signals in the inflammatory exudate of the superficial wound bed (Figure 2, A and B). The density of IL-8 mRNA$^+$ cells abruptly decreased toward the nonnecrotic underlying dermis, and IL-8 mRNA expression was completely absent in the adjacent epidermis during all phases of wound healing. At day 1, nearly 20% of total dermal cells expressed message for IL-8 (Figure 3). The dense rim of expressing cells spatially correlated with the dense neutrophil accumulation, as revealed by immunohistological staining on serial sections (Figure 2, A, B, and E). After
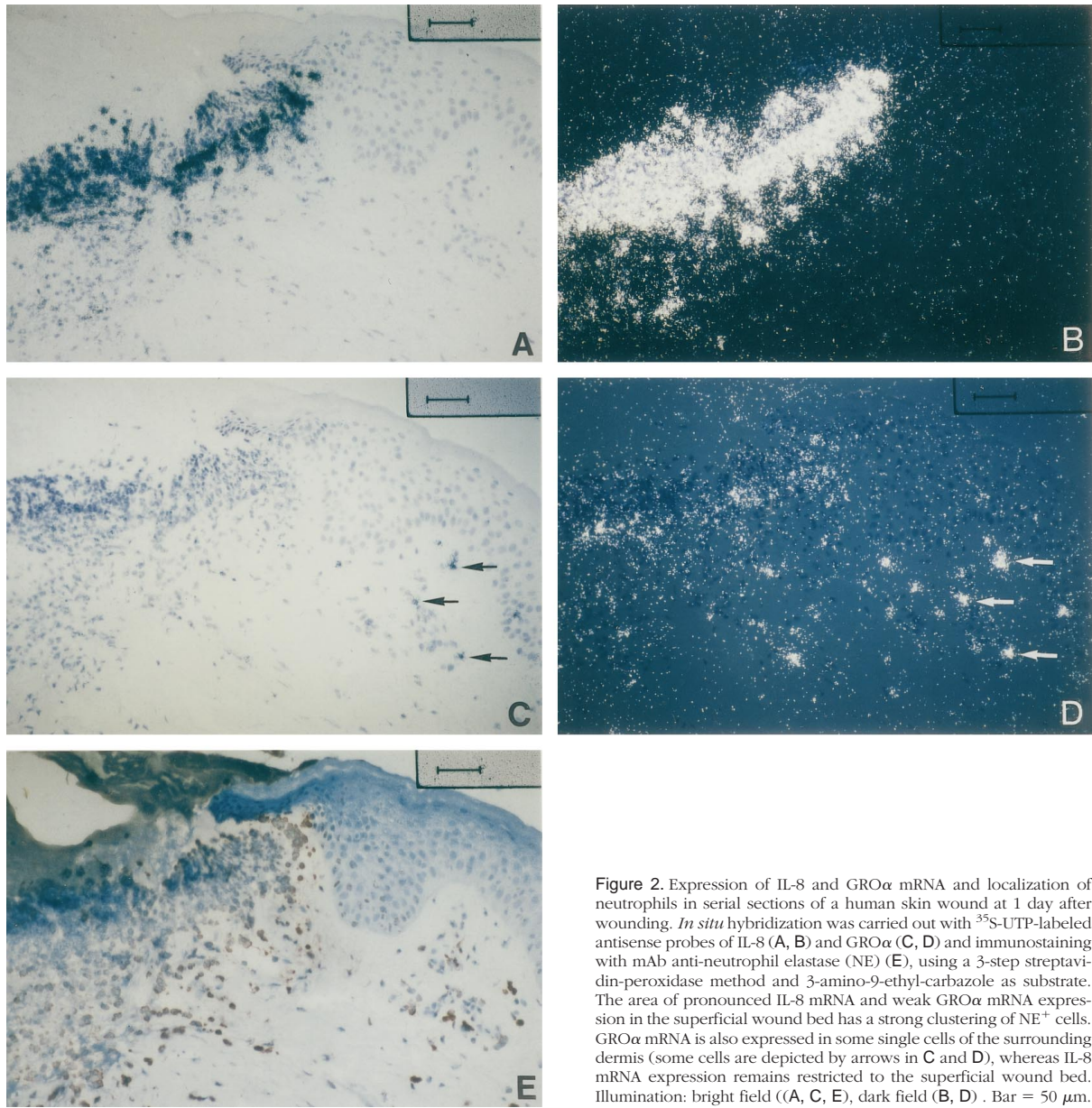
Figure 2. Expression of IL-8 and GROα mRNA and localization of neutrophils in serial sections of a human skin wound at 1 day after wounding. *In situ* hybridization was carried out with ^{35}S-UTP-labeled antisense probes of IL-8 (**A, B**) and GROα (**C, D**) and immunostaining with mAb anti-neutrophil elastase (NE) (**E**), using a 3-step streptavidin-peroxidase method and 3-amino-9-ethyl-carbazole as substrate. The area of pronounced IL-8 mRNA and weak GROα mRNA expression in the superficial wound bed has a strong clustering of NE$^+$ cells. GROα mRNA is also expressed in some single cells of the surrounding dermis (some cells are depicted by arrows in **C** and **D**), whereas IL-8 mRNA expression remains restricted to the superficial wound bed. Illumination: bright field ((**A, C, E**), dark field (**B, D**) . Bar = 50 μm.

day 1, the signal for IL-8 message declined such that after day 4 (complete re-epithelialization in all patients evaluated), IL-8 message was below detectable levels (Figure 3). Surprisingly, the neutrophils and IL-8 signals persisted in the crust material above the newly built epidermis, whereas the corresponding region below the neoepidermis had no detectable neutrophils and IL-8 message. IL-8 message detected above the neoepidermis was not included in this evaluation, since IL-8 in the crust is unlikely to influence wound cell activation in the dermis. Expression of GROα mRNA colocalized with IL-8 mRNA expression in the superficial wound (Figure 2, C and D) and was maximal after day 1 (Figure 3). However, in the superficial rim GROα expression was significantly lower than IL-8 expression. In contrast to IL-8, mononuclear cells in the wound area below the surface, particularly those with perivascular localization, expressed

strong message for GROα (Figure 2, C and D, arrows). GROα expression was still detectable at day 10 in the dermal compartment, albeit at low levels (Figure 3). Because the GROα and IL-8 expression profiles overlapped only partially in the superficial wound region, nonspecific cross-hybridization of these two highly homologous C-X-C chemokines can be excluded. When serial sections were hybridized with ENA-78 antisense probes, specific signals could not be detected between day 1 and day 21, suggesting that ENA-78 is not relevant for neutrophil recruitment in our wound healing model (data not shown). In summary, expression of both IL-8 and GROα mRNA showed a strong correlation with the neutrophil infiltration within the first 4 days after wounding, suggesting that both C-X-C chemokines cooperatively regulate neutrophil chemotaxis during normal healing of incisional skin wounds.
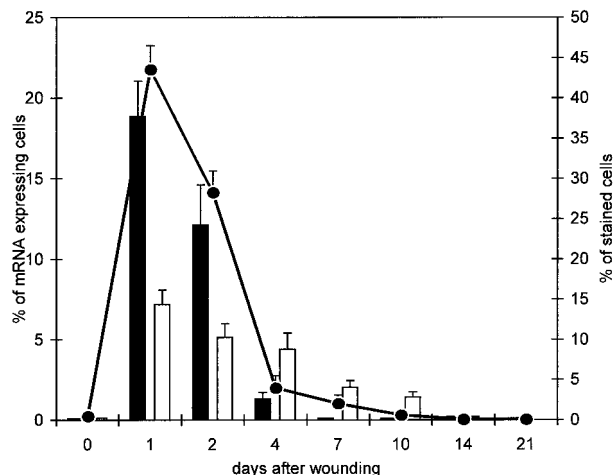
Figure 3. Quantification of IL-8 and GROα mRNA expressing cells and neutrophil infiltration during human skin wound healing. *In situ* hybridization for IL-8 (**filled bar**) and GROα (**empty bar**) mRNA expression was carried out with ^{35}S-UTP-labeled antisense RNA probes. The results are expressed as the mean percentage of specific mRNA-expressing cells per counting field (± SEM) of 4–14 lesion sections at each time point until day 21 after wounding. Neutrophils were identified by immunostaining with mAb anti-neutrophil elastase (●), using a 3-step streptavidin-peroxidase method and 3-amino-9-ethyl-carbazole as substrate. The results are expressed as the mean percentage of stained cells per counting field (± SEM) of 3–10 lesion sections for each time point until day 21 after wounding.

Selective Expression of MCP-1 mRNA during Healing of Incisional Skin Wounds Is Correlated with the Profile of Monocyte Infiltration

Wound macrophages exhibit both immunological and growth-promoting functions and thus comprise an essential cell population in cutaneous wounds. To discover which selected chemokines regulate macrophage accumulation during wound healing, we analyzed an extensive set of C-C chemokines with monocyte/macrophage attractant properties. The expression profiles of MCP-1, MCP-3, MIP1α, MIP-1β, I309, and RANTES were studied at days 0, 1, 2, 4, 7, 10, 14, and 21 after incision and consecutive healing by *in situ* hybridization using the corresponding sense and antisense probes. Expression levels of MCP-3, MIP-1β, I309, and RANTES were either very low or undetectable between day 0 and day 21 (data not shown). MIP-1α message was seen occasionally in the dermal compartment but its expression was marginal compared to the extensive recruitment of mononuclear cells in the wound (data not shown). In contrast to these C-C chemokines, MCP-1 mRNA expression was very extensive (Figure 4, A, B, and D–F) and surprisingly reached a maximum level at day 1, when nearly 20% of total cells expressed specific transcripts (Figure 5). The most noteworthy finding was the differential expression of MCP-1 in the dermal and epidermal compartment (Figure 4, D–F). Cell-associated MCP-1-specific signals were detected in the whole inflammatory focus of the wound area, especially around blood vessels. *In situ* hybridization does not allow the simultaneous demonstration of mRNA- and leukocyte-specific surface protein expression but, according to the distribution pattern and counterstaining,

MCP-1 message is most likely expressed by mononuclear cells (Figure 4, A, B, and D-F). Besides expression of MCP-1 by mononuclear cells in the dermis, we detected in every *in situ* hybridization focally abundant silver grain precipitates in the basal epidermal layer adjacent to the wound edge from day 2 to day 7. Interestingly, hybridization signals did not occur along the full length of the basal layer but were restricted to the part of vigorous basal proliferation as revealed by staining of serial sections with MiB-1 mAb (data not shown). After day 10, moderate MCP-1 mRNA expression was also detected in the basal layer of the newly built acanthotic neoepidermis (Figure 4, D-F). The strong basal expression of MCP-1 correlated spatially with a strong dermal accumulation of macrophages. There was also a strong correlation between the percentages of MCP-1-expressing cells and CD68$^+$ macrophages at all time points (Figure 5). This strongly suggests that MCP-1, which is synthesized by dermal mononuclear cells and basal keratinocytes at the wound edge, is a dominant monocyte chemoattractant during wound healing, for none of the other transcripts tested (MCP-3, MIP-1α and β, I309, or RANTES) could be detected.

Expression of the Chemokines Mig, IP-10, and MCP-1 in Normal Healing of Incisional Wounds Is Associated with Lymphocyte Recruitment

Recent data suggest that lymphocytes are not only immunological effector cells but also capable of producing growth factors, and thus may contribute to regeneration after tissue injuries.[6,7] In our wound healing model, lymphocytes were present in relatively high numbers and constituted the greatest leukocyte subgroup at day 14 after wounding (Figure 1). Currently, C-X-C chemokines[18,19,24,47] and C-C chemokines[33] are both considered to be lymphocyte attractants at least *in vitro*. As demonstrated above, MCP-3, MIP-1α and β, I309, and RANTES are expressed at low levels and so are not likely to be relevant for monocyte or lymphocyte trafficking. Therefore, we concentrated our study on the analysis of MCP-1, IL-8, GROα, and additional chemokines with lymphocyte-attractant properties, namely IP-10 and Mig. In the initial period of healing (day 1–4), lymphocytes were found mainly at the same sites as macrophages and MCP-1 mRNA expression. In contrast, the pattern of IL-8 mRNA expression was completely disparate, whereas GROα message was detected in singly distributed cells within foci of macrophage and lymphocyte accumulation. After day 4, hybridization of serial sections with IP-10 or Mig antisense (but not sense) probes as well as immunostaining for CD3 expression revealed a strong spatial correlation. In every instance we discovered foci with expression of IP-10 and Mig mRNA, the latter always at significantly higher levels (Figure 6, A and B), at clusters of lymphocytes (Figure 6C). At day 10, Mig mRNA expression reached a maximum level (7.3 ± 3.2% of total cells) which afterwards slowly declined. At day 21, 5 ± 4.7% of total cells were still Mig mRNA$^+$. A similar coincidence between lymphocyte accumulation and Mig/
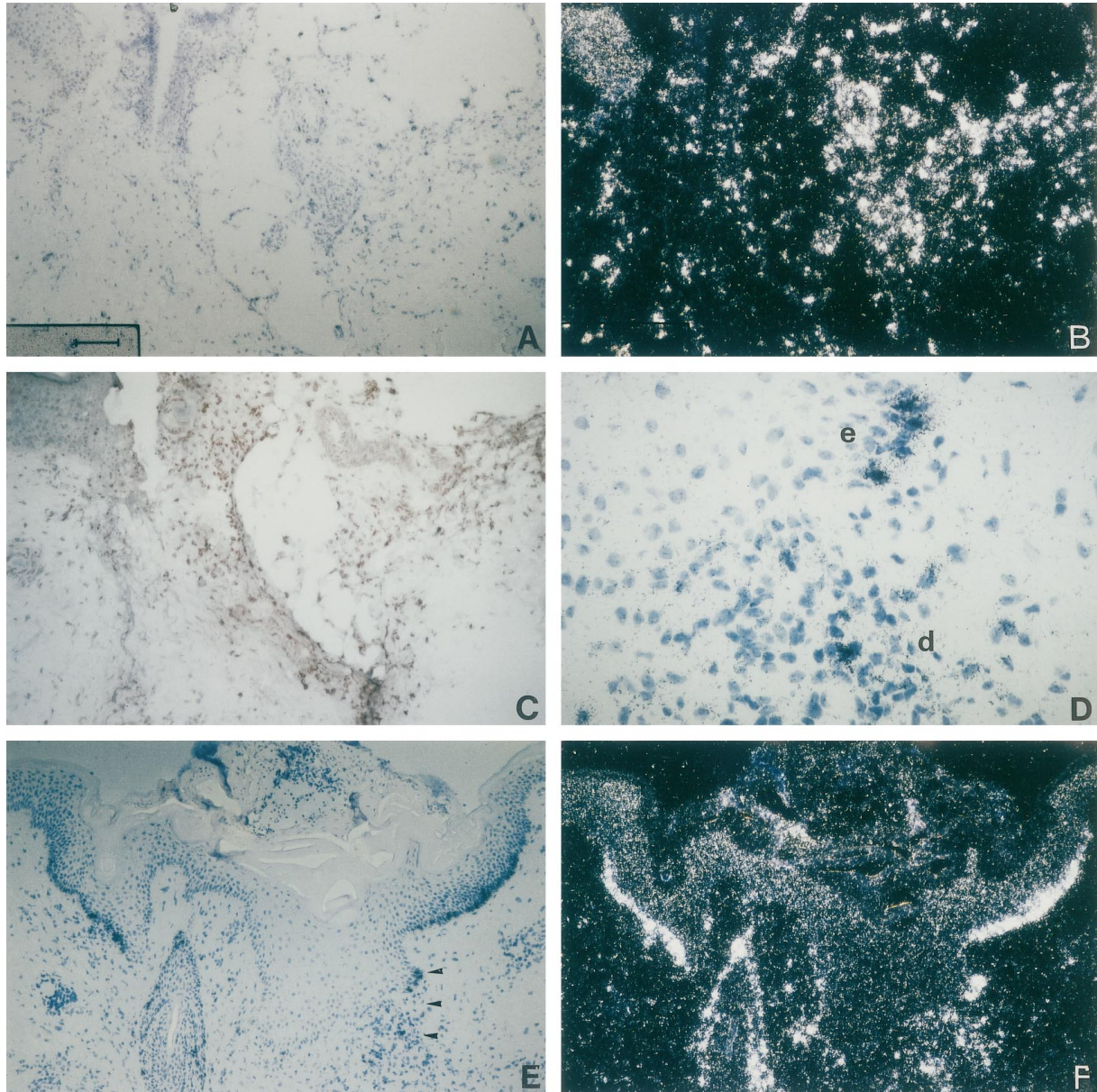
Figure 4. Expression of MCP-1 mRNA and localization of CD68^{+} monocytes/macrophages in serial sections of human skin wounds at 1 and 10 days after wounding. *In situ* hybridization was carried out with ^{35}S-UTP-labeled antisense probes of MCP-1 (**A, B, D, E, F**), and immunostaining with mAb anti-CD68 (**C**), using a 3-step streptavidin-peroxidase method and 3-amino-9-ethyl-carbazole as substrate. **A-C**: serial sections of an incisional human wound at the first day after wounding. Strong MCP-1 expression (**A, B**) in the wound area correlates with an accumulation of CD68^{+} macrophages (**C**). **D-F**: serial section of an incisional human wound 10 days after wounding. At day 10, MCP-1 is strongly expressed in keratinocytes of the basal layer of the hyperproliferative epidermis surrounding the wound (**E, F**). The area marked by arrowheads in **E** is shown in higher magnification (**D**) to demonstrate expression of MCP-1 in both infiltrating cells in the dermis (d) and in keratinocytes (e = epidermis). Illumination: bright field (**A, C, D, E**); dark field (**B, F**). Bar = 100 μm (**A, B, C, E, F**); bar = 25 μm (**D**).

IP-10 mRNA expression could not be detected for other chemokines, indicating that at a later stage of wound healing, these two chemokines are important for the persistence of lymphocyte recruitment. According to the expression pattern of IP-10 and Mig, macrophages are most likely to be the producers of both lymphoattractant chemokines. In summary, in both the time course experiments and the location of chemokine expression, we observed the presence of lymphocytes and MCP-1 expression in the early phase and IP-10/Mig expression in the later phase of wound healing.

MCP-1 mRNA Expression Is Paralleled by MCP-1 Immunoreactivity

Detection of soluble mediators *in situ*, in particular chemokines with binding to extracellular matrix components, is considered unreliable and troublesome. In the first days, immunohistochemical labeling using chemokine-specific mAbs and antiserum was hampered by a high background staining, possibly due to fibrin/fibrinogen. At day 4 and afterwards, the strong expression of MCP-1 mRNA (Figure 7A) was paralleled by MCP-1 immunore-
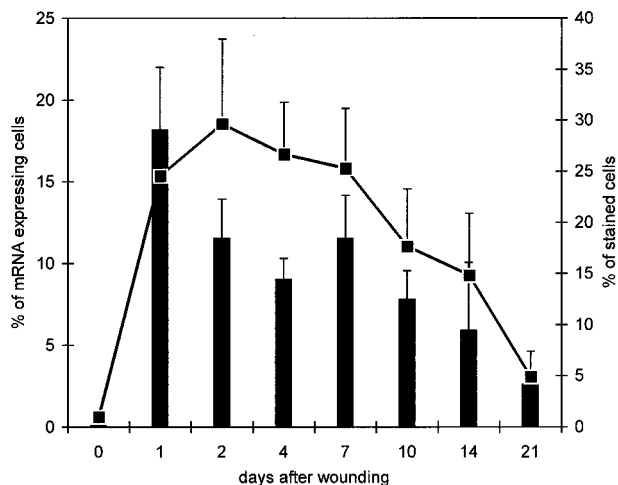
Figure 5. Quantification of MCP-1 mRNA-expressing cells and infiltration of CD68⁺ cells during human skin wound healing. *In situ* hybridization for MCP-1 (**filled bar**) mRNA expression was carried out with ³⁵S-UTP-labeled antisense RNA probes. Results are expressed as the mean percentage of MCP-1 mRNA expressing cells per counting field (± SEM) of 4–9 lesion sections at each time point until day 21 after wounding. Macrophages were identified by immunostaining with mAb anti-CD68 (■), using a 3-step strepta-vidin-peroxidase method and 3-amino-9-ethyl-carbazole as substrate. The results are expressed as the mean percentage of stained cells per counting field (± SEM) of 4–9 lesion sections for each time point until day 21 after wounding.

activity (Figure 7B), indicating translation of MCP-1 message into protein. Similar spatial and temporal correlation between mRNA expression patterns and chemokine immunoreactivity could be detected only for Mig and to a lesser extend IP-10 whereas the other chemokines with low mRNA expression levels (MIP-1α, RANTES) were not traceable by immunohistochemistry *in situ* (data not shown). In summary, except the early nonspecific immunoreactivity when staining for GROα and IL-8 at day 1 to 4, strong expression of MCP-1 and Mig/IP-10 mRNA were paralleled by a corresponding immunoreactivity indicating, that detected chemokine mRNA expression is translated to immunoreactive protein.

Initial Wound Neoangiogenesis Is Associated with High Levels of IL-8 and GROα Expression

Data are accumulating that IL-8 and GROα exhibit angiogenic properties *in vivo*[48,49] that are inhibited by IP-10 and Mig.[49] Because these angiogenic and angiostatic chemokines are highly expressed in our wound healing model, we compared chemokine expression levels with the numbers of immunohistochemically stained vessels counted in randomly selected regions of the wound. The density of vessels initially increased and remained constant after day 4. The expression levels of IL-8 and GROα clearly correlated with a delayed increase in vascularization, whereas expression levels of Mig and IP-10 did not reveal a corresponding correlation. In contrast to the increasing number of Mig/IP-10⁺ cells after day 4, vessel density remained constant.

Discussion

Recruitment of inflammatory cells to the wound site for immunological surveillance and production of growth factors is considered an essential process for wound healing.[1,3] However, little is known about the signals that regulate the regio-specific immigration of these cells in human cutaneous wounds. In the present study, we directed our attention to chemokines, which have the unique potential to activate and selectively guide various leukocyte subtypes to specific microanatomical sites of
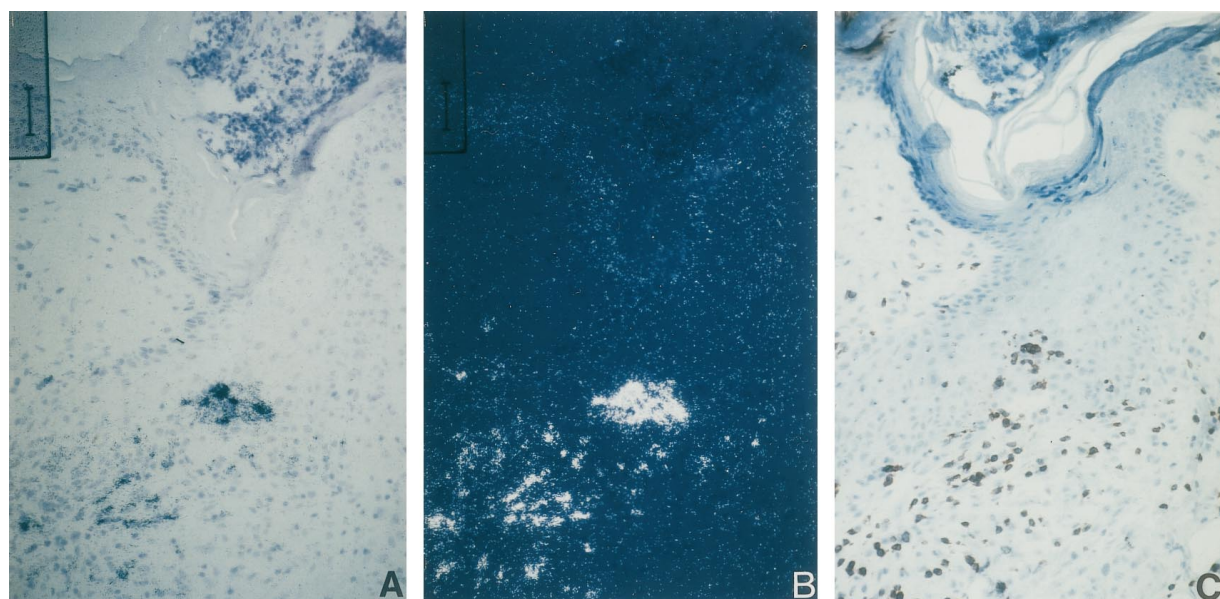

Figure 6. Focal expression of Mig mRNA coincides with the presence of CD3⁺ lymphocytes during the wound healing process. *In situ* hybridization was carried out with ³⁵S-UTP-labeled antisense probes of Mig (**A**, **B**) and immunostaining with mAb anti-CD3 (**C**), using a 3-step streptavidin-peroxidase method and 3-amino-9-ethyl-carbazole as substrate. **A-C**: serial sections of an incisional human wound 7 days after wounding. Mig mRNA-specific signals (**A**, **B**) are located mainly in the dermis and are associated with infiltrates of CD3⁺ lymphocytes (**C**). Illumination: bright field (**A**, **C**), dark field (**B**). Bar = 50 µm.

may exhibit multiple functions; most importantly, IL-8 attracts and activates neutrophils. A similar correspondence between IL-8 expression and neutrophil accumulation has been demonstrated in psoriasis, in which neutrophils also accumulate at sites of focal IL-8 expression.[42,51] Moreover, in both inflammatory conditions neutrophils produce IL-8 themselves and thus may enhance their own recruitment. The rapid accumulation of neutrophils after wounding may be accelerated by chemotactic substances such as N-formylmethionyl peptides derived from bacterial proteins and complement products.[1] However, their chemoattractant properties are not leukocyte subtype-specific and therefore, unlike IL-8 or GROα, they cannot explain the very selective band-like arrangement of neutrophils. The simultaneous but differential expression of IL-8 and GROα favors the concept that both C-X-C chemokines are in part involved in different steps of neutrophil recruitment via two different receptors, CXCR1 and CXCR2, respectively. This has been suggested for neutrophil trafficking from skin vessels to the upper epidermis in psoriasis lesions[42] and more recently for neutrophil accumulation in occluded blood vessels.[52] The vessel-associated expression of GROα in the absence of detectable IL-8 message may facilitate neutrophil diapedesis. The cooperative expression of GROα and IL-8 in the superficial wound bed supports further neutrophil migration to the wound surface along an ascending gradient. Thus, initial desensitization of the CXCR2 through GROα may be overcome through stimulation of neutrophils via the IL-8-specific CXCR1.[53] In addition to its neutrophil chemoattractant properties, IL-8 also directly stimulates keratinocyte migration and proliferation, as recently demonstrated by Michel et al and Tuschil et al.[54,55] In our wound healing model, IL-8 is expressed exactly along the denuded wound surface where keratinocytes migrate from the free edge of the adjacent epidermis. With complete wound closure, IL-8 expression subsides. The question of how IL-8 influences the phenotypic alter-
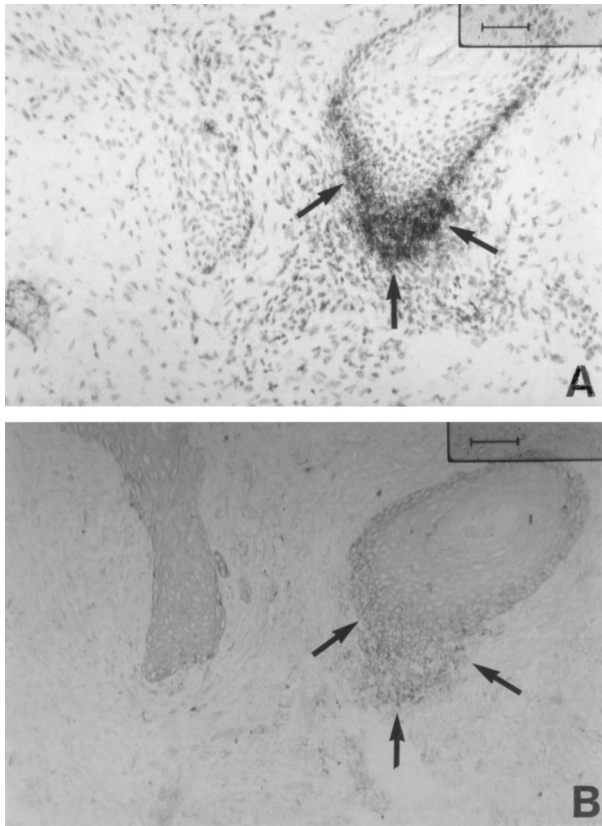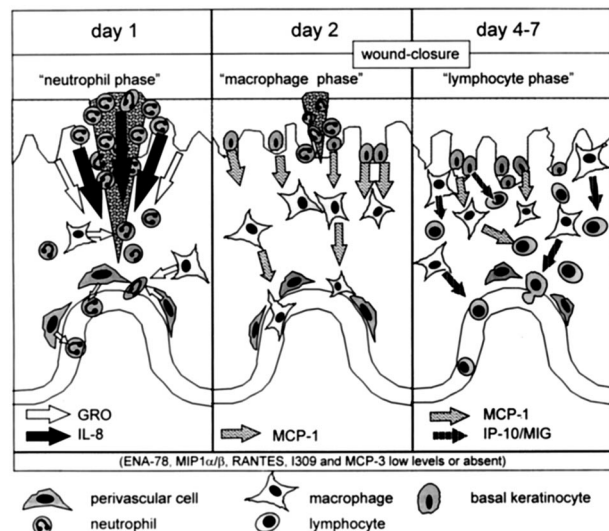

Figure 7. Expression of MCP-1 mRNA and localization of MCP-1 immunoreactivity in serial sections of human skin wounds at day 7 after wounding. *In situ* hybridization was carried out with ^{35}S-UTP-labeled antisense probes of MCP-1 (**A**), and immunostaining with mAb anti-MCP-1 (**B**), using a 3-step streptavidin-peroxidase method and 3-amino-9-ethyl-carbazole as substrate. **A, B**: serial sections of an incisional human wound at 7 days after wounding. Strong MCP-1 mRNA expression (**A**) in the wound area correlates with MCP-1 immunoreactivity (**B**) as depicted by arrows. In addition, there is homogenous (although weaker) nonspecific staining of the epidermis. Bar = 50 μm.

skin wounds during different phases of tissue repair. Using incisional adult skin wounds, our *in situ* findings indicate that migration and accumulation of the major leukocyte subtypes in wounds (neutrophils, monocytes/macrophages, and lymphocytes) is dynamically regulated by changing sets of chemokines. The first wave of immigration at day 1 is dominated by neutrophils, which migrate to the denuded wound surface. This migration correlates temporally and spatially with IL-8 and GROα mRNA expression, whereas the migration of macrophages is observed after strong expression of MCP-1 from day 2 onward. Lymphocyte migration is initially paralleled by MCP-1 expression and then after 4 days by Mig and IP-10 expression. The data are summarized in a diagram (Figure 8) demonstrating the intensity, location, and time course of chemokine expression and the recruitment of the corresponding target cells.

Peak levels of IL-8 at day 1 indicate that expression of this chemokine is rapidly up-regulated within a short time after wounding. Although *in vitro* data indicate that IL-8 is produced by a variety of cells present in the skin,[50] its expression in cutaneous wound healing is restricted to those cells which line the uppermost part of the wound, namely macrophages and neutrophils. IL-8, therefore,

Figure 8. Schematic drawing of the time course of chemokine-mediated recruitment of leukocyte subsets during normal healing of incisional human wounds.

ations of those keratinocytes which undergo metamorphosis and horizontal locomotion has so far not been investigated. Notably, the phenotype of migrating wound epidermal cell is similar to that observed in psoriatic skin. Expression of the CXCR2, recently reported in the proliferative population of keratinocytes of the wound edge,[39] and the proximity of high IL-8 levels and (to a lesser extent) GROα may also stimulate keratinocyte growth. Our data are in accordance with the data from Nanney et al[39] on burn wounds with respect to GROα expression. We also demonstrate that IL-8 participates in the regulation and interconnection of neutrophil inflammation and growth stimulation. The latter aspect is particularly interesting in light of the discovery of the angiogenic properties of both IL-8 and GROα.[48,49] The time course of strong IL-8 expression correlates with an increase in vessel numbers within the wound area between days 1 and 4. Whether IL-8 acts by a direct or indirect angiogenic mechanism remains to be elucidated and depends on whether sprouting vessels express the two IL-8-specific chemokine receptors CXCR1 and CXCR2.

Taken together, our data support the concept that GROα and particularly IL-8 are important and early mediators at different levels of the cytokine cascade during human skin wound healing. They may act as mediators of neutrophil inflammation in the early catabolic phase as well as stimulators of re-epithelialization and neoangiogenesis in the anabolic phase of wound repair.

In our cutaneous wound model, neutrophil accumulation is followed by the immigration of monocytes/macrophages. Maximum levels of MCP-1, which trigger macrophage recruitment, are reached by day 1 and slowly decline thereafter. Despite the capacity of resident dermal cell species (eg, microvascular endothelial cells and dermal fibroblasts) to produce a variety of C-C chemokines on stimulation *in vitro*,[56] the expression of all other chemokines tested in our human model (MCP-3, MIP-1α, Mip-1β, I309, and RANTES) is quiescent.

In addition to the observation that *in vitro* data on chemokine expression by resident cells of the skin are not relevant *in vivo*, our data also strongly indicate that knowledge about murine wound healing cannot easily be transferred to human wound healing. Unlike murine wound repair, in which MIP-1α has been suggested as a critical chemoattractant for macrophages,[36] the corresponding human chemokine is not detectable and thus not relevant to macrophage recruitment in human wounds.

Moreover, data from our human model indicates that basal keratinocytes of the adjacent epidermis contribute significantly to the inflammatory network in human wound repair by producing MCP-1, which has not been observed in murine skin wound healing.[38] As in psoriasis, MCP-1 mRNA in wounded skin tissue is strongly expressed in those basal keratinocytes which are hyperproliferative.[41] Therefore, it is tempting to speculate that MCP-1 may indirectly stimulate growth through the stimulation of recruited macrophages to produce growth factors such as PDGF, bFGF, TGFα, or TGFβ.[5] To test this hypothesis, we stimulated freshly isolated macrophages *in vitro* with various concentrations of MCP-1. However, we could not identify a significant stimulatory capacity of

MCP-1 for growth factor production in macrophages (unpublished observations). Therefore, our data suggest the function of MCP-1 in human skin wounds appears to be primarily the chemoattraction and activation of monocytes and macrophages which are afterwards stimulated by other signals to produce growth-promoting cytokines.

Whereas the role of neutrophils and macrophages is well established in wound healing,[1–3,5] lymphocytes have been discussed mostly in the context of an antigen-specific immune response. Because lymphocytes are also capable of producing growth factors[6,7] and are present in high numbers during the whole period of healing, even constituting the major leukocyte subpopulation after day 14, it is most likely that they actively influence the processes of tissue repair and remodeling. In our wound healing model, the chemokines MCP-1, Mig, and IP-10 are both T-cell attractant and highly expressed at sites of lymphocyte accumulation. We cannot exclude the possibility that other recently discovered lymphocyte attractants such as pulmonary and activation-regulated chemokine,[57] thymus and activation-regulated chemokine,[58] or lymphotactin[59] may contribute to the pronounced lymphocyte accumulation, especially between days 1 and 4 when Mig and IP-10 expression is absent. Mig and IP-10 are not only lymphocyte-dedicated chemokines; they also inhibit endothelial cell chemotaxis and angiogenesis induced by IL-8 or bFGF.[49] The fact that vascularity increases until day 4 but remains constant afterward, despite the presence of growth factors such as bFGF and PDGF, suggests that angiostatic properties of local factors can prevent unlimited vessel growth without blocking other repair processes involved in wound healing. Mig and IP-10 fulfill this criterion, for they can inhibit both endothelial cell chemotaxis and angiogenic activities of growth factors such as IL-8 and FGF. The relatively late appearance of Mig and IP-10 would thus preclude an angiostatic milieu at the early phase of wound healing. Because Mig and IP-10 are inducible by IFNγ[20,23] whereas synthesis of MCP-1, IL-8, and GROα is stimulated mainly by TNFα and IL-1,[10] the differential chemokine expression profiles may reflect a high expression of TNFα and IL-1 in the early phase and a delayed expression of IFNγ in the late phase of wound healing.

Our data on chemokines in adult human wound healing demonstrate that expression of different chemokines is tightly regulated during an ongoing, continuously changing inflammatory reaction and thus may contribute to the phase-specific recruitment of leukocyte subsets. Because skin wound healing is an ideal model for the study of inflammatory reactions with sequential participation of neutrophils, macrophages, and lymphocytes, our data on chemokine expression may also be relevant to other diseases such as bacterial infections. In adult skin wound healing, the interplay of GROα, IL-8, Mig, IP-10, and MCP-1 not only influences the targeting process of leukocyte subsets, it also (and more importantly) coordinates the inflammatory reaction of wound repair mechanisms. One can envision that particular chemokines might be used as phase-specific therapeutic agents in the regulation of wound repair.

Acknowledgments

References

1. Clark RAF: Basics of cutaneous wound repair. J Dermatol Surg Oncol 1993, 19:693–706

2. Clark RAF: The Molecular and Cellular Biology of Wound Repair. New York and London, Plenum Press, 1996

3. Martin P: Wound healing: aiming for perfect skin regeneration. Science 1997, 276:75–81

4. Brown EJ, Goodwin JL: Fibronectin receptors of phagocytes: characterization of the arg-gly-asp binding proteins of human monocytes and polymorphnuclear leukocytes. J Exp Med 1988, 167:777–793

5. Bennett NT, Schultz GS: Growth factors and wound healing. Am J Surg 1993, 165:-737

6. Blotnick S, Peoples GE, Freeman MR, Eberlein TJ, Klagsbrun M: T lymphocytes synthesize and export heparin-binding epidermal growth factor-like growth factor and basic fibroblast growth factor, mitogens for vascular cells and fibroblasts: differential production and release by CD4$^+$ and CD8$^+$ T cells. Proc Natl Acad Sci USA 1994, 91:2890–2894

7. Iida N, Haisa M, Igarashi A, Pencev D, Grotendorst G: Leukocyte-derived growth factor links the PDGF and CXC chemokine families of peptides. FASEB J 1996, 10:1336–1345

8. Frenette PS, Wagner DD: Adhesion molecules part II: blood vessels and blood clotting. N Engl J Med 1996, 335:43–45

9. Subramaniam M, Saffaripour S, Van De Water L, Frenette PS, Mayadas TN, Hynes RO, Wagner DD: Role of endothelial selectins in wound repair. Am J Pathol 1997, 150:1701–1709

10. Oppenheim JJ, Zachariae COC, Mukaida N, Matsushima K: Properties of the novel proinflammatory supergene "intercrine" cytokine family. Annu Rev Immunol 1991, 9:617–648

11. Schroeder JM, Christophers E: Identification of C5a $_{des\ arg}$ and an anionic neutrophil-activating peptide (ANAP) in psoriatic scales. J Invest Dermatol 1986, 87:53–58

12. Yoshimura T, Matsushima K, Oppenheim JJ, Leonard EJ: Neutrophil chemotactic factor produced by lipopolysaccharide (LPS)-stimulated human blood mononuclear leukocytes: partial characterization and separation from interleukin 1 (IL 1). J Immunol 1987, 139:788–793

13. Baggiolini M, Dewald B, Moser B: Interleukin-8 and related chemotactic cytokines-CXC and CC chemokines. Adv Immunol 1994, 55:97–179

14. Anisowicz A, Bardwell L, Sager R: Constitutive overexpression of a growth-regulated gene in transformed Chinese hamster and human cells. Proc Natl Acad Sci USA 1987, 84:7188–7192

15. Richmond A, Balentien E, Thomas HG, Flaggs G, Barton DE, Spiess J, Bordoni R, Francke U, Derynck R: Molecular characterization and chromosomal mapping of melanoma growth stimulatory activity, a growth factor structurally related to β-thromboglobulin. EMBO 1988, 7:2025–2033

16. Walz A, Burgener R, Car B, Baggiolini M, Kunkel SL, Strieter RM: Structure and neutrophil-activating properties of a novel inflammatory peptide (ENA-78) with homology to interleukin 8. J Exp Med 1991, 174:1355–1362

17. Clark-Lewis I, Schumacher C, Baggiolini M, Moser B: Structure-activity relationships of interleukin-8 determined using chemically synthesized analogs. J Biol Chem 1991, 266:23128–23134

18. Larsen CG, Anderson AO, Appella E, Oppenheim JJ, Matsushima K: The neutrophil-activating protein (NAP-1) is also chemotactic for T lymphocytes. Science (Wash DC) 1989, 243:1464–1466

19. Jinquan T, Frydenberg J, Mukaida N, Bonde J, Larsen CG, Matsushima K, Thestrup-Pedersen K: Recombinant human growth-regulated oncogene-α induces T lymphocyte chemotaxis. J Immunol 1995, 155:5359–5368

20. Farber JM: A macrophage mRNA selectively induced by γ-interferon encodes a member of the platelet factor 4 family of cytokines. Proc Natl Acad Sci USA 1990, 87:5238–5242

21. Farber JM: HuMIG: a new human member of the chemokine family of cytokines. Biochem Biophys Res Commun 1993, 192:223–230

22. Liao F, Rabin RL, Yannelli JR, Koniaris LG, Vanguri P, Farber JM: Human Mig chemokine: Biochemical and functional characterization. J Exp Med 1995, 182:1301–1314

23. Luster AD, Ravetch JV: Biochemical characterization of a γ-interferon-inducible cytokine (IP-10). J Exp Med 1987, 166:1084–1097

24. Taub DD, Lloyd AR, Conlon K, Wang JM, Ortaldo JR, Harada A, Matsushima K, Kelvin DJ, Oppenheim JJ: Recombinant human interferon-inducible protein 10 is a chemoattractant for human monocytes and T lymphocytes and promotes T cell adhesion to endothelial cells. J Exp Med 1993, 177:1809–1814

25. Loetscher M, Gerber B, Loetscher P, Jones SA, Piali L, Clark-Lewis I, Baggiolini M, Moser B: Chemokine receptor specific for IP10 and Mig: structure, function, and expression in activated T-lymphocytes. J Exp Med 1996, 184:963–969

26. Farber JM: Mig and IP-10: CXC chemokines that target lymphocytes. J Leukoc Biol 1997, 61:246–257

27. Yoshimura T, Robinson EA, Tanaka S, Appella E, Kuratsu J-I, Leonard EJ: Purification and amino acid analysis of two human glioma-derived monocyte chemoattractants. J Exp Med 1989, 169:1449–1459

28. Matsushima K, Larsen CG, DuBois GC, Oppenheim JJ: Purification and characterization of a novel monocyte chemotactic and activating factor produced by a human myelomonocytic cell line. J Exp Med 1989, 169:1485–1490

29. Wolpe SD, Davatelis G, Sherry B, Beutler B, Hesse DG, Nguyen HT, Moldawer LL, Nathan CF, Lowry SF, Cerami A: Macrophages secrete a novel heparin-binding protein with inflammatory and neutrophil chemokinetic properties. J Exp Med 1988, 167:570–581

30. Sherry B, Tekamp-Olson P, Gallegos C, Bauer D, Davatelis G, Wolpe SD, Masiarz F, Coit D, Cerami A: Resolution of the two components of macrophage inflammatory protein 1, and cloning and characterization of one of those components, macrophage inflammatory protein 1 β. J Exp Med 1988, 168:2251–2259

31. Miller MD, Krangel MS: The human cytokine I-309 is a monocyte chemoattractant. Proc Natl Acad Sci USA 1992, 89:2950–2954

32. Schall TJ, Jongstra J, Dyer B, Jorgensen J, Clayberger C, Davis MM, Krensky AM: Human T-cell specific molecule is a member of a new gene family. J Immunol 1988, 141:1018–1025

33. Loetscher P, Seitz M, Clark-Lewis I, Baggiolini M, Moser B: Monocyte chemotactic proteins MCP-1, MCP-2, and MCP-3 are major attractants for human CD4+ and CD8$^+$ T lymphocytes. FASEB J 1994, 8:1055–1060

34. Taub DD, Proost P, Murphy WJ, Anver M, Longo DL, Van Damme J: Monocyte chemotactic protein-1 (MCP-1), -2 and -3 are chemotactic for human T lymphocytes. J Clin Invest 1995, 95:1370–1376

35. Baggiolini M, Dahinden CA: CC chemokines in allergic inflammation. Immunol Today 1994, 15:127–133

36. DiPietro LA, Burdick MD, Low QE, Kunkel SL, Strieter RM: MIP-1α as a critical macrophage chemoattractant in murine wound repair. J Clin Invest 1998, 101:1693–1698

37. Iida N, Grotendorst G: Cloning and sequencing of a new gro transcript from activated human monocytes: expression in leukocytes and wound tissue. Mol Cell Biol 1990, 10:5596–5599

38. DiPietro LA, Polverini PJ, Rahbe SM, Kovacs EJ: Modulation of JE/MCP-1 expression in dermal wound repair. Am J Pathol 1995, 146:868–875

39. Nanney LB, Mueller SG, Bueno R, Peiper SC, Richmond A: Distributions of melanoma growth stimulatory activity or growth-regulated gene and the interleukin-8 receptor in human wound repair. Am J Pathol 1995, 147:1248–1260

40. Ritter U, Moll H, Bröcker E-B, Velazco O, Becker I, Gillitzer R: Differential expression of chemokines in patients with localized and diffuse cutaneous American leishmaniasis. J Infect Dis 1996, 173:699–709

41. Gillitzer R, Wolff K, Tong D, Mueller C, Yoshimura T, Hartmann AA, Stingl G, Berger R: MCP-1 mRNA expression in basal keratinocytes of psoriatic lesions. J Invest Dermatol 1993, 101:127–131

42. Gillitzer R, Ritter U, Spandau U, Goebeler M, Bröcker E-B: Differential expression of GRO-α and IL-8 mRNA in psoriasis: A model for neutrophil migration and accumulation in vivo. J Invest Dermatol 1996, 107:778–782

43. Goebeler M, Toksoy A, Spandau U, Engelhardt E, Bröcker E-B,

Gillitzer R: The C-X-C chemokine Mig is highly expressed in the papillae of psoriatic lesions. J Pathol 1998, 184:89–95

44. Schroeder JM, Gregory H, Young J, Christophers E: Neutrophil-activating proteins in psoriasis. J Invest Dermatol 1992, 98:241–247

45. Sambrook J, Fritsch EF, Maniatis T: Molecular Cloning. Cold Spring Harbor, NY, Cold Spring Harbor Laboratory Press, 1989

46. Angerer LM, Stoler M, Angerer RC: In situ hybridization with RNA-probes. In In situ hybridization: Application to CNS. Edited by K Valentin, J Eberwine, and J Barchas. New York, Oxford University Press, 1987, pp 42–70

47. Taub DD, Anver M, Oppenheim JJ, Longo DL, Murphy WJ: T-lymphocyte recruitment by interleukin-8 (IL-8). J Clin Invest 1996, 97:1931–1941

48. Koch AE, Polverini PJ, Kunkel SL, Harlow LA, DiPietro LA, Elner VM, Elner SG, Strieter RM: Interleukin-8 as a macrophage-derived mediator of angiogenesis. Science 1992, 258:1798–1801

49. Strieter RM, Polverini PJ, Kunkel SL, Arenberg DA, Burdick MD, Kasper J, Dzuiba J, Damme JV, Walz A, Marriott D: The functional role of the 'ELR' motif in CXC chemokine-mediated angiogenesis. J Biol Chem 1995, 270:27348–27357

50. Schroeder JM: Cytokine networks in the skin. J Invest Dermatol 1995, 105:20S–24S

51. Kulke R, Todt-Pingel I, Rademacher D, Rowert J, Schroeder JM, Christophers E: Co-localized overexpression of GRO-α and IL-8 mRNA is restricted to the suprapapillary layers of psoriatic lesions. J Invest Dermatol 1996, 106:526–530

52. Ludwig A, Petersen F, Zahn S, Goetze O, Schroeder JM, Flad H-D, Brandt E: The CXC chemokine neutrophil-activating peptide-2 induces two distinct optima of neutrophil chemotaxis by differential

interaction with interleukinn-8 receptors CXCRR1, and CXCRR2. Blood 1997, 90:4588–4597

53. Premack BA, Schall T: Chemokine receptors: gateways to inflammation and infection. Nature 1996, 2:1174–1178

54. Michel G, Kemeny L, Peter RU, Beetz A, Ried C, Arenberger P, Ruzicka T: Interleukin-8 receptor-mediated chemotaxis of normal human epidermal cells. FEBS Lett 1992, 305:241–243

55. Tuschil A, Lam C, Haslberger A, Lindley I: Interleukin-8 stimulates calcium transients and promotes epidermal cell proliferation. J Invest Dermatol 1992, 99:294–298

56. Goebeler M, Yoshimura T, Toksoy A, Ritter U, Bröcker E-B, Gillitzer R: The chemokine repertoire of human dermal microvascular endothelial cells and its regulation by inflammatory cytokines. J Invest Dermatol 1997, 108:445–451

57. Hieshima K, Imai T, Baba M, Shoudai K, Ishizuka K, Nakagawa T, Tsuruta J, Takeya M, Sakaki Y, Takatsuki K, Miura R, Opendakker G, Van Damme J, Yoshie O, Nomiyama H: A novel human CC chemokine PARC that is most homologous to macrophage-inflammatory protein-1α/LD78α and chemotactic for T lymphocytes, but not for monocytes. J Immunol 1997, 159:1140–1149

58. Imai T, Yoshida T, Baba M, Nishimura M, Kakizaki M, Yoshie O: Molecular cloning of a novel T cell-directed CC chemokine expressed in thymus by signal sequence trap using Epstein-Barr virus vector. J Biol Chem 1996, 271:21514–21521

59. Kennedy J, Kelner GS, Kleyensteuber S, Schall TJ, Weiss MC, Yssel H, Schneider PV, Cocks BG, Bacon KB, Zlotnik A: Molecular cloning and functional characteritation of human lymphotactin. J Immunol 1995, 155:203–209